Neurocomputing 640 (2025) 130323

Contents lists available at ScienceDirect

Neurocomputing

journal homepage: www.elsevier.com/locate/neucom

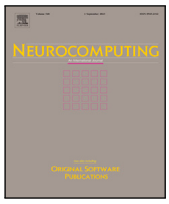

Semantization of memories in a hippocampal–cortical spiking neural network

Federico D'Alba [a,b,*], Nilay Kushawaha [a,b], Lorenzo Fruzzetti [c], Pier Stanislao Paolucci [d], Egidio Falotico [a,b]

[a] The BioRobotics Institute, Scuola Superiore Sant'Anna, Pontedera, Italy
[b] Department of Excellence in Robotics and AI, Scuola Superiore Sant'Anna, Pisa, Italy
[c] CNR - Consiglio Nazionale Ricerche, Pisa, Italy
[d] Istituto Nazionale di Fisica Nucleare (INFN), Roma, Italy

ARTICLE INFO

Communicated by Q. Zheng

Keywords:
System memory consolidation
Spiking neural networks
Continual learning
Dendritic Integration Theory

ABSTRACT

The human brain consolidates episodic memories into more semantic representations during sleep, enabling the continuous integration of new knowledge. This transformation is supported by hippocampal replays, which triggers a reactivation and reshaping of synaptic connections in the neocortex. In this study, we developed a plastic spiking neural network of Leaky Integrate-and-Fire (LIF) neurons to simulate the interaction between the hippocampus, perceptual neocortical areas, and neocortical regions responsible for processing semantic and contextual information. The model operates in two learning phases: first, the network encodes new experiences as episodic memories; then, during a sleep-like phase, hippocampal reactivation propagates to the neocortex. Crucially, the model leverages the apical mechanisms recently proposed by the experimentally grounded Dendritic Integration Theory (DIT) to modulate the activity of neural assemblies during both learning and replay. We evaluated the model on continual learning tasks, including split and rotational MNIST, and further demonstrated its practical applicability by training and testing it on sensory data from a soft pneumatic gripper in a dynamic robotic environment.

1. Introduction

Adaptation in an ever-changing world is a critical feature for survival and evolution. In human beings, adaptation arises from the consolidation of memories, which enables us to accumulate knowledge over time and retain past information. As we build knowledge over time, our brain must encode novel and useful information, integrating it into our existing knowledge structure while discarding redundant elements. But how does our brain accomplish this remarkable feat? It relies on system memory consolidation, a process where memories initially encoded in the hippocampus are reorganized and transferred to the neocortex for long-term storage. The exact mechanisms of system consolidation are still unknown but there exist mainly three theories. The 'standard consolidation theory' [1] states that upon hippocampal reactivation and co-activation with neocortical ensembles, memories are gradually transferred to the latter. In this theory, memories become independent from the hippocampus and depend solely on the neocortex. On the other hand 'Multiple Trace Theory' [2] proposes that the hippocampus is always involved in the storage and retrieval of memories and that they do not become independent from it. In this theory, each newly acquired memory creates a 'trace' and that semantization happens through an overlapping of these traces in the neocortex. Finally, 'Trace Transformation Theory' [3] proposes a dynamic interplay between neocortex and hippocampus in which memories are still transferred to the neocortex but they do not lose their dependence on the hippocampus. For what concern this paper, we stick with the standard consolidation theory and we focus on the active system consolidation processes that are in great part reviewed in [4]. We would like to emphasize that our choice to adopt the Standard Consolidation Theory was not based on a claim of superiority over the Multiple Trace Theory or the Trace Transformation Theory. Instead, it was a modeling choice, driven by the specific focus and objectives of our study. The Standard Consolidation Theory offers a well-established framework that aligns closely with the active system consolidation processes we aimed to explore. In the following, we introduce the main experimental evidences involving active system consolidation that we used as basic inspiration to develop our model. Memories are initially encoded in both the neocortex [5] and the hippocampus [6,7] (Fig. 1 left panels).

* Corresponding author at: The BioRobotics Institute, Scuola Superiore Sant'Anna, Pontedera, Italy.
E-mail address: federico.dalba@santannapisa.it (F. D'Alba).

https://doi.org/10.1016/j.neucom.2025.130323
Received 22 October 2024; Received in revised form 17 February 2025; Accepted 19 April 2025
Available online 3 May 2025

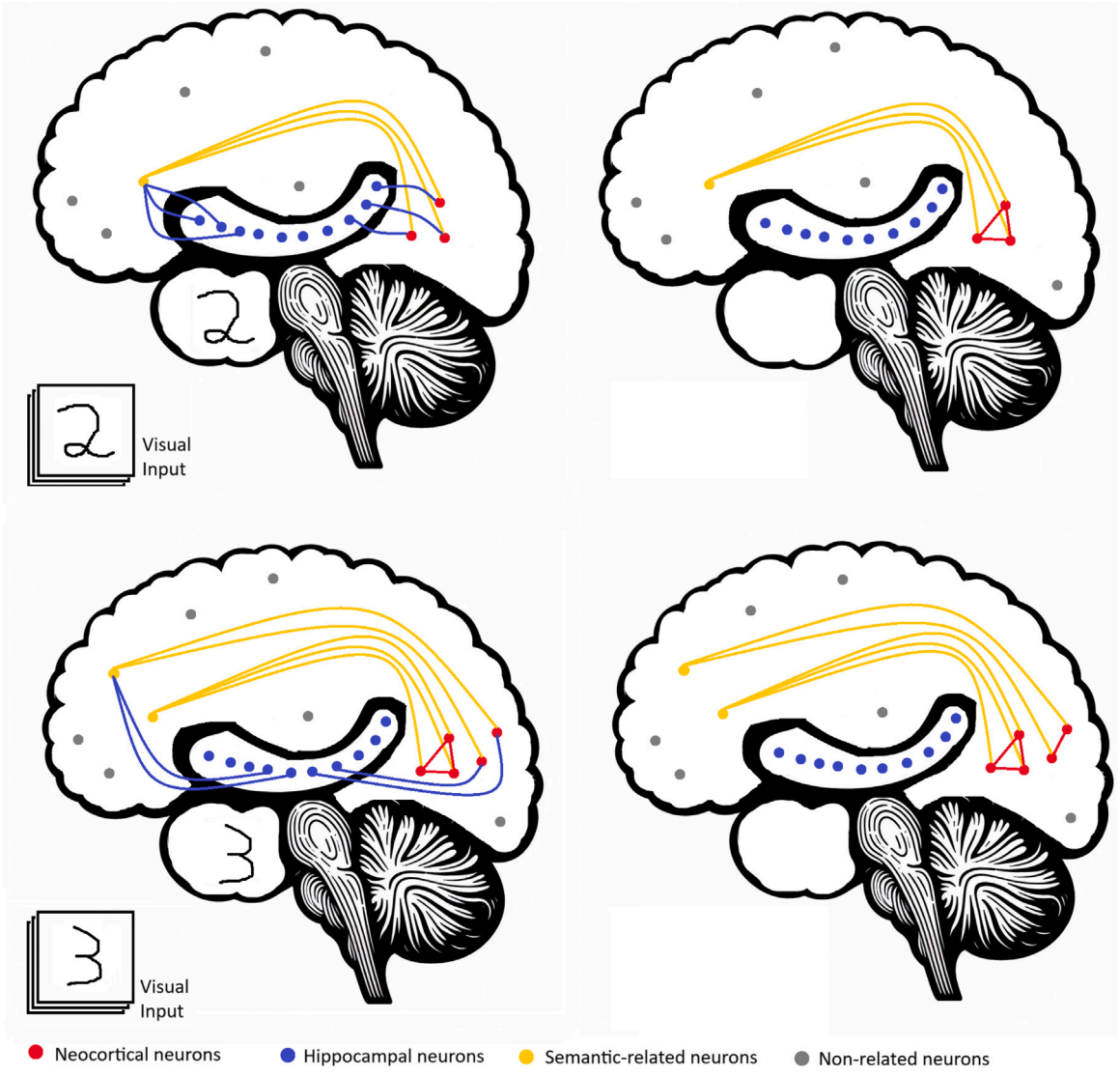

Fig. 1. The figures on the left depict neural connections during wakeful learning, while those on the right illustrate the connections after sleep. When encountering novel stimuli, the brain encodes different elements of the experience across various regions, with the hippocampus linking these components to form episodic memories. During sleep, hippocampal networks are reactivated, reinforcing connections in other brain regions that share related semantic content.

Here, the hippocampus functions as a fast learner, capturing episodic features after a singular occurrence; however, these representations exhibit limited stability [8]. In contrast, the neocortex is considered a gradual learner, forming long-lasting representations only after repeated exposures [9]. Our cortex possesses billions of neurons and trillion of synapses, yet under typical physiological conditions, only a small part of this vast network is active simultaneously. Conscious perception is associated with the activation of a fraction of neurons, which are connected across different cerebral areas and within the same regions. These neurons represent both the internal and external worlds at various levels of abstraction. A systemic perspective on these processes is provided by the Integrative Theory of Consciousness [10].

This theory highlights the importance of the Dendritic Integration Theory (DIT) as an essential cellular mechanism. DIT is experimentally grounded in the apical mechanisms experimentally demonstrated by [11] in wakefulness, dreaming [12], and unconscious states [13]. In such a systemic theory, an essential component is the interplay between contextual signals from other areas, which strongly modulate the local activity of a "cooperative cortical neuron" [14]. Throughout the day, our brain acquires a small fraction of new information. According to the DIT, new evidence is collected in the perisomatic zones of pyramidal neurons and is amplified if it coincides with contextual information projected from areas of the brain at higher or similar hierarchical levels. This supports a fundamental characteristic of the cerebral cortex: its capacity to link elements of perceived experience with internal representations of the world. Information about the external world (sensory input, bottom-up stream) flows in a feed-forward manner, establishing a baseline frequency of neuronal firing. Whereas feedback inputs (top-down stream) reach the most electrically remote region of the pyramidal neuron's distal tuft dendrites, they significantly increase the neuron's firing rate only if – and only if – they coincide with the feed-forward flow. However, when feedback inputs arrive outside this coincidence detection window, they have minimal influence on spike generation in the axon [11]. In this context, the apical signal provides either contextual or predictive information to modulate neural activity in a specific area [11]. As everyday experiences are encoded in our brain, diverse cortical regions encapsulate different components of these experiences. The hippocampus links all these cortical regions together, leading to the formation of an episodic memory [6,7] (Fig. 1 left panels). During sleep, the hippocampal neuronal representations undergo recurrent reactivation [15], propagating across the associated cortical memory components and facilitating the gradual transfer of memory representations from the hippocampus to the neocortex [8,16]. This reactivation triggers synaptic consolidation processes, reinforcing

memory representations in the neocortex and facilitating their integration into pre-existing long-term semantic memories [17], or promoting the emergence of novel categories [18,19] (Fig. 1 right panels). Importantly, the systems consolidation during sleep not only enhances the long-term stability of memories but also induces a reorganization of the connections that changes the representations of single episodic memories into more abstracted, gist-like, and long-term memories [17]. At the cellular level, this process involves a dynamic interplay of synaptic upscaling and downscaling within the ensembles hosting the memory representation. Some synaptic connections weaken, due to the system being embedded in a global downscaling process [20], while others maintain or increase their involvement, resulting in selective synaptic strengthening and upscaling [4,21]. Synaptic changes in our brain can be modeled by Spike-Timing-Dependent Plasticity (STDP). STDP is a concept in neuroscience that explores how the connections between neurons can change in strength over time. The key factor in STDP is the precise timing of spikes in the activity of connected neurons. STDP is based on the idea that the relative timing of spikes from the pre-synaptic and post-synaptic neurons determines whether a synapse is strengthened or weakened. If the pre-synaptic spike occurs just before the post-synaptic spike, the synapse is likely to strengthen, a phenomenon known as Long-Term Potentiation (LTP). Conversely, if the order is reversed, with the post-synaptic spike preceding the pre-synaptic spike, the synapse tends to weaken, leading to Long-Term Depression (LTD). This mechanism is considered a form of Hebbian learning, where the phrase "cells that fire together wire together" captures the essence of the process. Essentially, if a neuron consistently contribute to the activation of another, the connection becomes stronger [22]. However, traditional Hebbian learning neglects the synergistic cooperation of apical amplification mechanisms and novelty related neuromodulation. While neuromodulators communicate information related to novelty or reward, contextual signals carry the information about the current internal priors and expected semantic value of the incoming information. Their impact on synaptic plasticity proves to be valuable especially for determining the timing of creating new memories in response to sensory stimuli. Indeed our brain avoids the encoding of already consolidated stimuli [23]. To avoid the encoding of redundant information our brain makes use of novelty or reward signals [24]. Novelty could be encoded in the phasic activity of a neurotransmitter that gates synaptic plasticity [24], for instance, it could be represented by an increase of acetylcholine [25] or dopamine [26,27]. In this work, despite the particular kind of neuromodulator, we used the synaptic update rules proposed in [24].

The aim of this work is to construct a system memory consolidation spiking model where learning happens through the presence of a global neuromodulatory signal plus sparse and context/semantic specific signals. Thanks to memory consolidation processes, our brain is capable of integrating new information while retaining past knowledge. This enables to learn continually in a dynamic evolving environment by getting new knowledge but also consolidating the one previously acquired [28]. Therefore, we believe that it is essential for a memory consolidation model to be tested successfully on continual learning (CL) scenarios [29]. To reach this goal, we develop a spiking neural network of LIF neurons with a realistic range of parameters and with the following features: (i) Learning of novel experiences happens in specific assemblies thanks to the coincidence of the apical contextual signals and modulating attention (ii) Nightly replay of recently encoded memories (iii) Homeostatic effect of sleep (iv) Episodic memories are transformed into semantic memories (v) Decisions are made thanks to winner-take-all dynamics (vi) A two-step learning phase enables CL (vii) No need to specify a priori the number of classes to be learned. Our model integrates key experimental findings on active system consolidation, particularly the interactions between the hippocampus, neocortex, and the dendritic mechanisms described by the Dendritic Integration Theory (DIT). One crucial aspect of our approach is the role of apical dendrites in modulating neural activity. Experimental studies suggest that apical input—combining contextual priors and feed-forward sensory evidence—can induce high-frequency bursting in a subset of neurons. We incorporate this mechanism in both hippocampal and cortical areas by selecting specific neuronal subsets through the *projectors* U_{perc}, Λ_{sem}, and U_{cue} (see Fig. 2 and Table 2). This targeted modulation facilitates learning by enhancing firing rates in selected neurons. Additionally, our model accounts for the interaction between brain states and attention-dependent plasticity modulation. Experimental evidence supports the idea that neuromodulatory signals dynamically regulate synaptic plasticity, favoring different learning processes depending on the brain's state (e.g., wakefulness vs. sleep). This principle is embedded in our model through distinct learning phases: during wakeful learning, synaptic modifications occur based on sensory inputs, while during sleep-like replay, hippocampal activation reinforces cortical and input-cortical connections, leading to the gradual formation of semantic memories. By integrating these biologically inspired mechanisms, our model aims to capture the essential dynamics of active system consolidation, providing a simplified yet functionally relevant abstraction of hippocampal–cortical interactions. Therefore, the main contribution of this work can be summarized as follows:

1. We present a spiking neural network that models the interaction between the hippocampus and neocortex.
2. We implement a learning rule that leverages apical amplification mechanisms and the presence of neuromodulators and compare it with the classical STDP rule.
3. We evaluate the proposed model in four CL scenarios: Split MNIST, Rotated MNIST, CIFAR10, CIFAR100 and compared it with a PNN.
4. To demonstrate the practical applications of the proposed CL algorithm, we test it in a dynamic environment, specifically on a soft pneumatic gripper equipped with two force sensors and two flex sensors for object classification.

1.1. Related works

In the following, we will briefly introduce some of the most significant works related to this study. Specifically, we will introduce works that implemented a mechanism of semanticization or some form of consolidation during a sleep phase or modeled the role of apical-amplification mechanisms and neuromodulators in memory models.

In [30], they implemented sleep cycles to consolidate memories in a hippocampus–neocortex rate-based model. In [31], they investigated the mechanistic processes of system consolidation, but they did not consider any role for neuromodulators. In [32], they addresses memory consolidation based on the Synaptic Tagging and Capture (STC) hypothesis, focusing on synaptic-level dynamics. In contrast, our work models consolidation at the system level, emphasizing the transfer of memories between the hippocampus and neocortex. In [33], they proposed a new learning rule in a cortical network and showed that they could semanticize memories; however, they did not model the interaction between the hippocampus and neocortex. In [34], they modeled the transformation of episodic memories into semantic ones, but they used an artificial network and lacked biological plausibility. In [35], they developed a spiking hippocampus–neocortex model and investigated under which conditions a memory can be semanticized; however, they used a different STDP rule and a single neuron model and did not implement any homeostatic process to deal with different input intensities. In [36], they modeled the interaction between the hippocampus and neocortex through hippocampal replay but their model lacked a semanticization method, and therefore, their model could only recall memories but not generalize them. The work in [37] leverages graph theory to analyze the relationship between semantic memory structure and creativity. Their model represents semantic concepts as nodes and similarities as weighted edges. In contrast, our model consists of a network of Leaky Integrate-and-Fire (LIF) neurons,

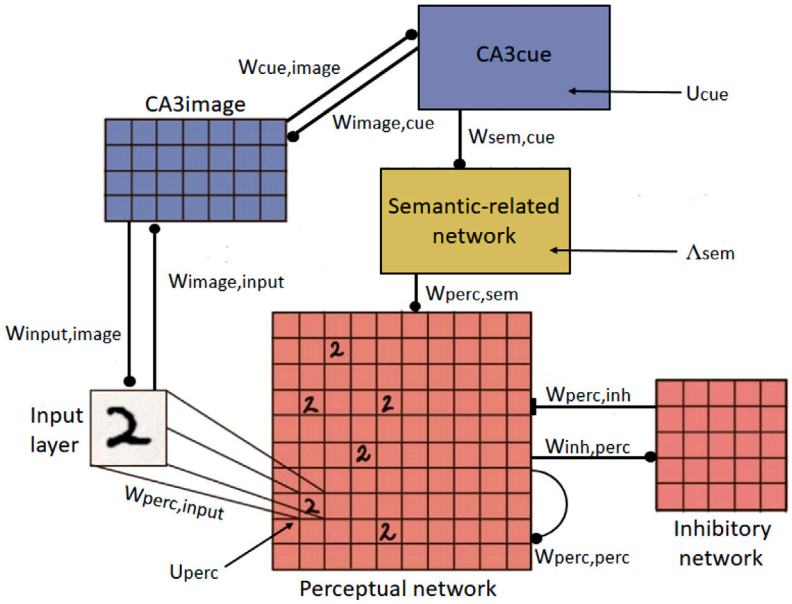

Fig. 2. Network's architecture. The hippocampus is colored in blue, the excitatory neuron of perceptual neocortex in red and the semantic cortical neuron in yellow.

Table 1
Summary of all synaptic matrices.

Synaptic matrix	Connectivity	Awake plasticity	Sleep plasticity
$W_{perc,input}$	all-to-all	Yes	Yes
$W_{image,input}$	one-to-one	No	No
$W_{input,image}$	one-to-one	No	No
$W_{cue,image}$	all-to-all	Yes	No
$W_{image,cue}$	all-to-all	Yes	No
$W_{sema,cue}$	all-to-all	Yes	No
$W_{perc,sema}$	all-to-all	Yes	No
$W_{perc,perc}$	all-to-all	No	Yes
$W_{perc,inh}$	$p = 0.5$	No	No
$W_{inh,perc}$	$p = 0.5$	No	No

Table 2
Brain-state and area-dependent projectors of unsupervised and semantic contextual signals.

Projectors	Awake training	Sleep	Classific.
U_{cue}	Yes	Random permutation	No
U_{perc}	Yes	No	No
Λ_{sema}	Yes	No	No

aiming to capture the semantization process. Unlike [37], our model learns features from a dataset and focuses on the dynamics of semantic-contextual interactions during memory consolidation. In [26], they showed the possible role of dopamine during nightly replay, but they did not model any interaction with the neocortex. Finally, in [18,19], they combined context and perception to consolidate representations in a thalamo-cortical spiking neural network, but they did not implement any interaction with the hippocampus. None of these proposed computational models combine the role of apical amplification mechanisms and neuromodulators in a memory consolidation model that includes hippocampal–cortical interaction.

In the next section, we will introduce the methods used to achieve our objectives. Specifically, we will introduce the network's architecture, the single neuron and synapse model, the neuromodulated STDP rule, and the training and testing procedure. In the Results section, we will show the homeostatic effect of the implemented sleep phase, the semanticization of memories, demonstrate that the implemented sleep phase can improve visual classification, and compare these results with a classical STDP rule. After that, we will evaluate the model on two CL scenarios, such as Split MNIST, where the model has to learn incrementally novel categories, and rotational MNIST, where the model has to learn from a non-stationary distribution. Furthermore we will show the performance of our model on data taken from a gripper. Finally, in the last section, we will discuss the results and talk about the possible future directions of the proposed model.

2. Methods

The simulations are conducted using the BRIAN2 simulator [38]. Equations are integrated using the 2nd order Runge–Kutta method. Hyperparameters are explored with a bayesian search algorithm [39]. In this section, we provide a description of the single neuron and synapse model, the network's architecture, outline the learning rules employed, and finally explain the training procedure.

2.1. Represented areas

The network (see Fig. 2) is composed by a very simplified version of the hippocampus, one excitatory and one inhibitory layer of the perceptual neocortex, an associative network abstracting other neocortical areas representing neural correlates of semantic and contextual information, and an input layer.

2.1.1. Input layer

The input layer is composed by 28×28 neurons(one neuron per image pixel). From now on, *input* will denote neurons of this area.

2.1.2. Perceptual neocortex

We will denote by *perc* and *inh* the excitatory and inhibitory neurons in the perceptual neocortex. The number of *perc* spiking neurons is correlated with the memory capacity of the model. It has been demonstrated [18,19] that an assembly composed of $G \approx 20$ neurons per memory provides an extremely robust representation and facilitates the spontaneous reactivation of individual memories during wake and sleep phases in neo-cortical models, but we will consider in this work the extreme (and more economic) case of setting $G = 1$ in the perceptual network. The number of *inh* spiking neurons is set to the classical

value of a quarter of the excitatory ones as in realistic cortical network. $W_{perc,inh}$ and $W_{inh,perc}$ connect random with a probability of connection of 50%. Excitatory–excitatory connections ($W_{perc,perc}$) are plastic (see Table 1) and are shaped by the hippocampus during the sleep phase, as illustrated in later sections.

2.1.3. Hippocampus

The architecture of the hippocampus is inspired by the work of [40] and comprises solely the CA3 area, that we modeled as composed by the CA3cue and CA3image subareas. Corresponding neurons are denoted as *cue* and *image*, respectively. Hippocampal *image* spiking neurons receive and project one-to-one ($W_{image,input}$ and $W_{input,image}$) connections from/to *input* neurons. $W_{cue,image}$ and $W_{image,cue}$, the connections between CA3image and CA3cue neurons are plastics and supporting an all-to-all connectivity, and thanks to the dynamics later described, after learning each episodic memory is represented by a single *cue* neuron. A single CA3cue can reactivate a specific image in CA3image during the sleep phase. Like for the cortex, we set the extreme case of only one *cue* neuron per experience. CA3cue targets also the semantic-related neocortex, through the $W_{sema,cue}$ synaptic matrix.

2.1.4. Semantic-contextual neocortex

This highly abstracted network represents the role of category-specific network like ATL or associative networks that can keep track of semantic knowledge [41]. It is represented by the *sema* array of non-interconnected spiking neurons. The number of *sema* neurons equals the number of semantic categories. Its primary function is to associate episodic memory with contextual or categorical information pertaining to the episode. This network receives all-to-all connections from all CA3cue episodic memories belonging to the same category trough the $W_{sema,cue}$ connectivity matrix. Each *sema* neuron projects one-to-many connections towards all neurons in the perceptual neocortical area belonging to the category it represents, through the $W_{perc,sema}$ matrix.

Table 1 summarizes the set of synaptic matrices connecting the area represented in the model, their connectivity and state dependent plasticity.

2.2. Examples, categories and modulation projectors

During the awake training we followed a modeling choice that has been introduced in [18,19] to capture basic features of the apical-mechanism [11] in network models composed by point-like neurons. Indeed, brain-state specific apical mechanisms are supported in biological networks by dedicated neural mechanisms [14]: during wakefulness, apical-amplification supports the detection of the temporal coincidence of perception (impinging on the perisomatic compartment) and time-specific contextual signals (reaching the apical compartment). Pyramidal neurons signal the coincidence detection by dramatically increasing their firing rate. This way it is possible a fast storage of individual experiences in neural groups of limited size. An accurate modeling of the phenomenon would require at least two-compartment neurons, e.g. [42,43]. In networks including single compartment neurons a basic approximation can be achieved by implementing a WTA dynamics while selecting different neural assembly through a time-dependent projector of input current (in this case U_{perc}) that represent the apical contextual signal.

In the model, the training happens on N examples for each of C semantic categories. Each example is numbered as $e_i, i \in \{0, \dots, E = NC - 1\}$. During the training, each example is presented for a time interval Δt_{train} followed by a silence period of duration Δt_{train}. The time associated to each example is denoted as $t_i, i \in \{0, \dots, E\}$. The first essential ingredients of our formulation are the U_{perc} and U_{cue} projectors. They represent time-dependent unsupervised apical signals projected by the other areas of the brain. Under the assumption that a complex brain never passes in the same state twice and that contextual inter-areal signals are extremely sparse, it is possible to abstract such unsupervised signal using Poissonian inputs $I(t_i, p_j)_{area,context}$ set to non-zero values by a projector $U(t_i, p_j)_{area} = \delta_{i,j}$. This way the time-dependent unsupervised contextual poison signal targets different time-specific (t_i) neural assemblies (p_j) in the perceptual cortical and hippocampal CA3Cue area inducing activity only on the assembly representing the episodic memory. Excitatory neurons in the *perc* area are also stimulated by an $I_{perc,stim}$ current trough the $W_{perc,input}$ matrix. *cue* neurons are also reached by the projection carried by $W_{cue,image}$. Images in *input* are copied to the hippocampal CA3image by the one to one connection $W_{image,input}$. In summary, U_{perc} modulates the creation of example specific rows in the synaptic matrix $W_{perc,input}$, while U_{cue} modulates the creation of episodic specific rows in the $W_{cue,image}$ synaptic matrix. Another ingredient is the category projector $\Lambda(e, c)_{sema}$. The Λ_{sema} projector abstracts the supervised component of the learning and represents the creation of categorical labels in the anterior semantic-contextual areas of the brain Λ_{sema} assumes the value 1 when the example e belongs to the semantic category c and 0 otherwise. Λ_{sema} modulates the activity of categorical neurons in the semantic cortex, shaping a $W_{sema,cue}$ synaptic matrix that has values different from zero only for synapses that connect *cue* neurons belonging to the same category of the neuron in *sema*. Also in this case we set the size of the categorical assembly to 1. During training, thanks to STDP, the simultaneous activity of example specific assemblies in the perceptual cortical area and category specific assemblies in the semantic network induces the spontaneous creation of a $W_{perc,sema}$ synaptic matrix that connects a categorical assembly in *sema* only to those *perc* neurons that represent examples belonging to the same category. Similarly, an attention and/or novelty projector α_e represents the neuromodulated information projected by other areas of the brain about the novelty or relevance of the proposed example. The novelty projector (α) can reach all neurons in a area. For simplicity, we will assume $\alpha_e \in 0, 1$, i.e., in this work an example is considered either interesting or non interesting. We summarize in Table 2) the brain-state specific activity of the above described projectors. They modulate Poissonian inputs I_{noise} to create local *contextual* signal targeting specific neural assemblies at different times in each area, resulting in a current $I_{projector}$ equal to $I(t_i, p_j)_{area,context} = U_{area,t_i,p_j} I_{noise}$.

2.3. Single neuron and synapse model

To simulate the dynamic of excitatory neurons in all areas, we used the leaky integrate-and-fire neuron. Neurons in the perceptual cortex include also an adaptive threshold to mimick biological spike frequency adaptation (SFA). The membrane potential v is described by:

$$\tau_m \frac{dv}{dt} = -(v - V_0) + R_m I \tag{1}$$

where I is the sum of all inter-areal and recurrent inputs (see Table 1), plus the signals imposed by the projectors (see Table 2). Here V_0 is the rest membrane potential, τ_m is the integration time of the membrane potential, V_{syn} is the reverse synaptic potential, R_m is the membrane resistance. When the neuron's membrane potential reach a value θ the neuron fires and its membrane potential is reset to V_{reset}. The variable θ follows a first-order differential equation. As the neuron fires, θ is increased by a value b, and after each spike, it returns to its resting value θ_0 with a decaying time constant τ_{th}. After the reset, the neuron is in its refractory period and it cannot fire again within few milliseconds. We chose a conductance-based model for the synapse in which synaptic currents are voltage dependents and the conductance temporal course is described by:

$$\tau_{syn} \frac{ds}{dt} = -s + w \sum^{pre} \delta(t - t^{pre}) \tau_m \tag{2}$$

Where τ_{syn} is the decay time, w is the weight of the connection between pre and post synaptic neuron and the sum on the r.h.s. runs over all

the pre-synaptic spike received by the post-synaptic neuron. Therefore, synaptic currents are described by:

$$I_{syn}(t) = s(t)(v(t) - V_{syn})g_{syn} \tag{3}$$

Where V_{syn} is the reversal synaptic potential and g_{syn} is the conductance related to a particular synaptic current. We modeled two kind of synaptic currents: AMPA and GABA which are respectively the excitatory neurotransmitter and the inhibitory one.

We used biologically plausible values of the parameters (see Table 3) for all the simulations performed in this work.

2.4. Learning rule

To model synaptic plasticity we use a three factor learning rule [24] in which the weight update can be described by a function H:

$$\frac{dw}{dt} = H(pre, post, M) \tag{4}$$

that depends on pre and post synaptic activity plus a neuromodulatory signal that modulates synaptic changes. In our model we defined a modulation function m that can depends on entering the *awake* or *sleep* state and on the *area* target neurons are belonging to.

In the following, x and y are $pre-$ and $post-$ synaptic traces left by neurons at each fire event. They decay as:

$$\tau_+ \frac{dx}{dt} = -x + \sum^{pre} \delta(t - t^{pre})\tau_+ \tag{5}$$

$$\tau_- \frac{dy}{dt} = -y + \sum^{post} \delta(t - t^{post})\tau_- \tag{6}$$

Synaptic updates can be summarized as follows: As post-synaptic neuron fires the weight w got an increment

$$w_+ = a_+(x(t)m(t) - tar) \tag{7}$$

While as pre-synaptic neuron fires the weight got a reduction

$$w_- = a_-y(t) \tag{8}$$

m represents the brain-state and area dependent neuromodulation. it follows the following differential equation:

$$\tau_n \frac{dm}{dt} = -m + W_{m,state} \sum^{post} \delta(t - t^{post})\tau_n \tag{9}$$

a_+ and a_- are the learning rates, W_{max} is the maximum value for the weights and tar is a parameter that helps to disconnect neurons that fires less as already introduced in [44]. $W_{m,state}$ represents the jump of the variable m at each post-synaptic activation and it depends on the brain-state (awake, sleep). We chose to use an additive rule because we noticed that it gave slightly better results after the hippocampal replay than the multiplicative rule. In this work a particular attention is dedicated to the identification of optimal values for the conductance g_c in:

$$I_{perc,sema}(t) = s(t)(v(t) - V_{syn,E})g_c \tag{10}$$

as well as of the value for $W_{m,state}$ in Eq. (9), and tar in Eq. (7). g_c, $W_{m,state}$ and tar are determined through bayesian optimization [39] in order to maximize the accuracy on a given validation set.

2.5. Training, sleep and classification

We trained and tested the network on the MNIST dataset and on gripper data. In this paragraph, we explain the training procedure for the MNIST dataset, while its adaptation to gripping is reported in Section 3.4. Each image is first deskewed, transformed into black and white, and then each active pixel is converted into a Poisson spike train with a rate of 63.5 Hz. Each training example is presented for 500 ms, during which plasticity (Section 2.4) shapes the synaptic

Table 3
Summary of the parameters and their respective units.

Parameters	Value	Unit
V_0	−70	mV
θ_0	−52	mV
b	20	mV
V_{reset}	−59	mV
$V_{syn,I}$	−70	mV
$V_{syn,E}$	0	mV
$R_{m,E}$	40	MΩ
$R_{m,I}$	50	MΩ
g_{syn}	1	nS
$\tau_{m,E}$	20	ms
$\tau_{m,I}$	10	ms
$\tau_{syn,E}$	2	ms
$\tau_{syn,I}$	5	ms
$\tau_{th,wake}$	1	ms
$\tau_{th,sleep}$	144	ms
τ_+	16.8	ms
τ_-	33.7	ms
τ_n	114	ms
a_+	0.0065	–
a_-	0.00071	–
W_{EonI}	1	–
W_{IonE}	2	–
$W_{max,neocortex}$	1	–
$W_{max,hippocampus}$	110	–
$W_{m,awake}$	0.1	–

matrices $W_{target,source}$ depicted in Fig. 2. The perceptual network operates under a hard Winner-Take-All dynamic. Winner-Take-All (WTA) dynamics refer to the behavior of networks of neurons where one neuron or a group of neurons suppresses the activity of others in the same network [22]. During training, one cortical neuron in the perceptual area is selected by the unsupervised time-dependent U_{perc} context projector. Simultaneously, the hippocampus encodes and stores the image in its recurrent CA3image < − > CA3cue connections. A single, identifiable neuron in the CA3cue network is activated, thanks to the effect of the unsupervised time-dependent U_{cue} projector. Connections between the CA3cue network and the semantic network are shaped thank to the information carried by Λ_{sema} projector. Notably, the connections between the semantic network and the perceptual neocortex spontaneously emerge thanks to the plasticity detecting the subsets of *sema* and *perc* neurons simultaneously active during the presentation of each example. During the sleep phase, images stored in the hippocampus are replayed multiple times through the input layer. This is achieved by randomly stimulating neurons in the CA3cue network for 50 ms intervals. Activation of a single neuron in CA3cue leads to the reactivation of the image via the CA3image network. The activation of hippocampal neurons is then propagated towards neocortical neurons and the semantic-related network encoding the same label. Consequently, while images are replayed, neurons in the neocortex associated with the same label as the replayed image receive sparse contextual signals from the semantic-related network.

The synaptic tagging from the hippocampus serves two functions: it facilitates connections among neurons associated with the same label and experience, and it enables the redistribution of input-cortex synaptic connections. During the classification phase, all synaptic connections are fixed, and images are presented to the neocortex. Due to the connections with a common inhibitory layer, only groups with higher activity continue to fire. Classification is achieved through population coding, with the population exhibiting the highest average firing rate deemed the winner. Finally, we chose to compare our model's performance with that of a Progressive Neural Network (PNN) [45]. We selected PNN because, like our model, it falls into the "dynamic architecture" category of continual learning methods. In PNN, a new column is added for each experience to encode new data, similar to our approach, where additional neurons are introduced at each learning stage. Being a conventional artificial neural network rather

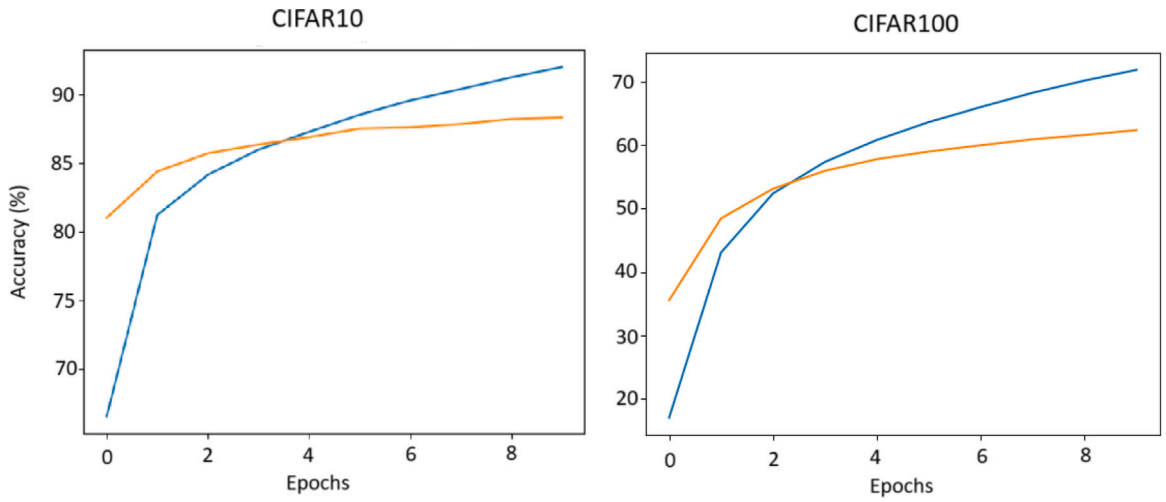

Fig. 3. Finetuning of VGG19 on CIFAR10 (left) and CIFAR100 (right). **Blue line**: Training Accuracy. **Orange line**: Validation Accuracy.

than a spiking one, PNN has the advantage of potentially achieving significantly higher performance given a sufficient amount of data. However, its major drawback is the requirement to specify a task identity (task ID) during the test phase. The task ID determines which column is used for prediction, artificially boosting accuracy compared to our method. This reliance on explicit task identification, however, makes PNN less suitable for real-world applications. We trained PNN on the same dataset as our model, using the same preprocessing.

2.6. VGG19 feature extraction and fine-tuning

To process the CIFAR10 and CIFAR100 datasets, we employed VGG19 [46] as a feature extractor, leveraging its pre-trained convolutional layers to obtain meaningful image representations. The dataset was divided into three subsets: 30,000 samples for fine-tuning, 10,000 for validation, and 10,000 for training the spiking network. To enhance generalization and mitigate overfitting, we applied data augmentation techniques such as random cropping and horizontal flipping. We initialized VGG19 with ImageNet pre-trained weights, freezing all convolutional layers except for the last four, which were fine-tuned on CIFAR10 and CIFAR100 to adapt the model to the specific domain. Additionally, we included an upsampling layer to match the original VGG19 input size and improve feature extraction. The model was trained using cross-entropy loss and optimized with Adam, applying a learning rate scheduler to facilitate convergence. VGG19 overfitted after a few epochs (Fig. 3); therefore, for feature extraction, we trained it for 3 epochs on CIFAR10 and 2 epochs on CIFAR100. After fine-tuning, we extracted features using a Global Average Pooling (GAP) layer, producing a 512-dimensional feature vector per image. This vector was normalized and thresholded at 0.5 to convert it into a spike representation, where values above the threshold were encoded as spike trains firing at 250 Hz, while lower values were set to zero.

3. Results

3.1. Sleep improves visual classification

Firstly, we partition a fraction of the MNIST training dataset to serve as a validation set. Subsequently, we train the network using 500 excitatory cortical neurons, with each neuron encoding a single image presented during the training phase (50 images per label). Fig. (4A) illustrates the episodic memory stored in a single hippocampal neuron for a specific image. During the sleep phase, CA3cue neurons are stimulated to re-present the images learned during training, thereby reactivating cortical neurons associated with the same image labels (Fig. 5). Fig. 4B demonstrates how the sleep phase redistributes input-cortical connection weights, strengthening common features among images of the same label while weakening non-common features.

We attempt to optimize parameters specifically for the wake phase but find that optimal accuracy is achievable over a wide range of parameters, particularly by varying the neuromodulatory strength ($W_{m,wake}$) and the maximum input-cortico weight (W_{max}). We then choose $W_{max} = 1$ and $W_{m,wake} = 0.1$ as reported in Table 3. Subsequently, we address the challenge of parameter optimization for the sleep phase, where multiple parameters influence outcomes. To streamline this process, we focus on parameters unrelated to computation time—namely, $W_{m,sleep}$ (neuromodulatory weight change), g_c (neuronal excitability due to context-specific signals), and tar (rate of disconnection). Through Bayesian optimization involving these parameters, we identify a parameter set that achieves an average accuracy of 90% on a small validation set (500 images per class, drawn from the training set). The parameter ranges for the Bayesian search are as follows: $W_{m,sleep}$: (0, 0.1), g_c: (1 nS, 100 ns), and tar: (0, 10). The optimal parameters obtained from the Bayesian search are: $W_{m,sleep} = 0.0045$, $g_c = 9.9$ nS, and $tar = 1$. Upon testing the model with these optimized parameters, we achieve an average accuracy of 86%, representing a significant improvement of over 5σ from the average accuracy attained without incorporating the sleep phase, which stands at 75% as depicted in Fig. (5C).

Furthermore, we conduct a comparison between the proposed rule and the STDP rule utilized in [44]. As depicted in Fig. (5C), the classical STDP rule marginally enhances visual classification, resulting in a slight increase in average accuracy by a few points. However, this improvement is not comparable to the enhancements achieved with our proposed rule.

3.2. Homeostasis effect of sleep

Digits within the MNIST dataset exhibit varying numbers of pixels between images belonging to different labels. For example, an image classified as 'zero' typically contains around 150 activated pixels, while an image classified as 'one' averages around 80 activated pixels. To prepare these images for presentation to the network, we transform each pixel into a Poisson spike train with a specified rate. Consequently, this results in significantly different input intensities, leading to distinct cortical activity patterns for zeros and ones. Often, this manifests as dominance of neurons encoding zeros during the classification phase.

This model incorporates two homeostasis mechanisms. The first involves an adaptive threshold, whereby a neuron that has recently fired will exhibit reduced firing in the near future. The second mechanism

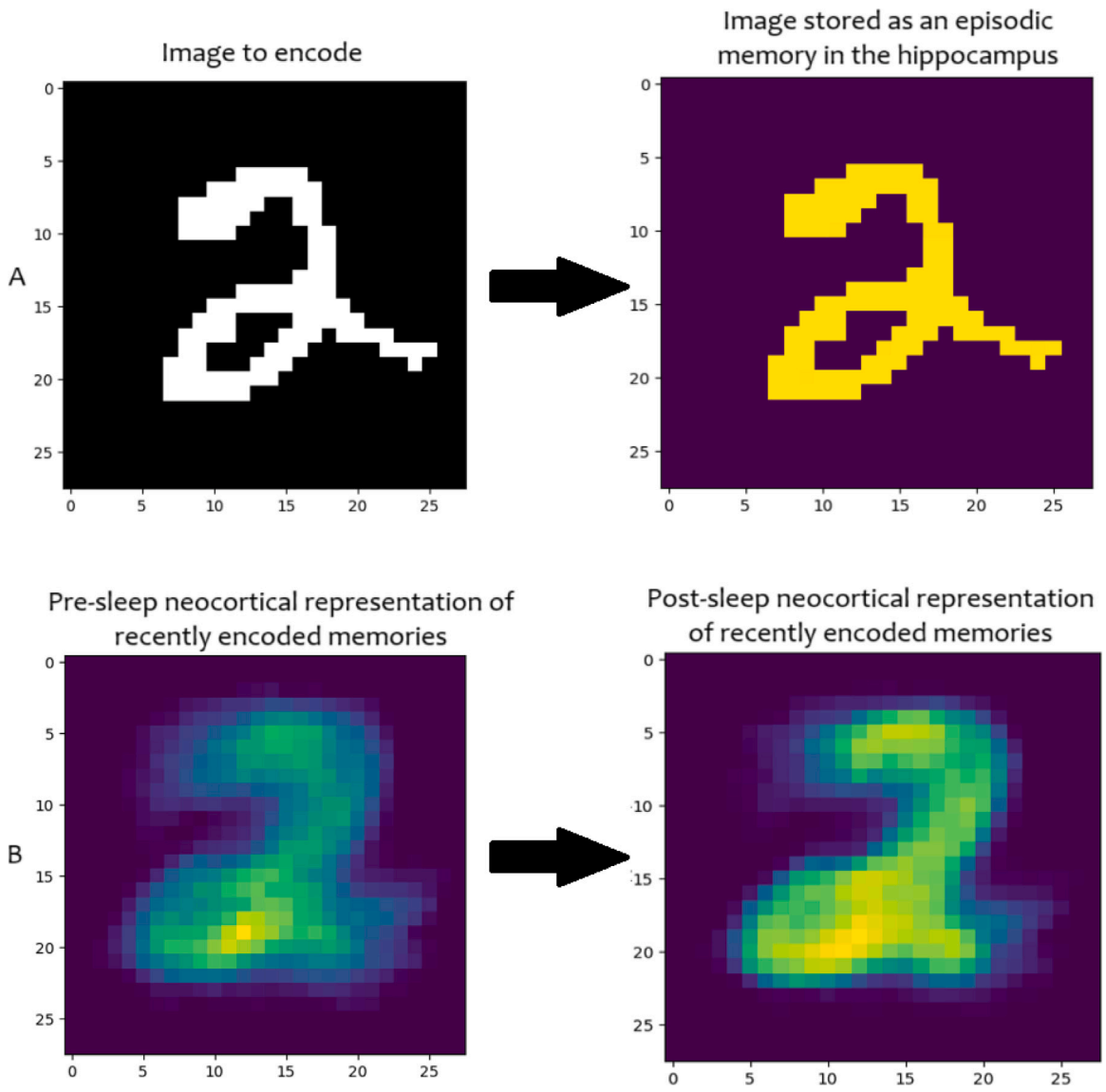

Fig. 4. **A**: During the wake phase, image data are encoded as episodic memories in the hippocampus. The figure on the right represent the weights between the cue specific neuron in CA3cue and CA3image neurons after the encoding. **B**: On the left there are the overlapped neocortical weights of 50 neurons that encoded 50 images. On the right is showed the same figure but after the sleep phase. Common features between fifty twos are emphasized while non-common features are weakened and that led to the creation of a semantic memory.

involves a global downscaling of synaptic strengths during the sleep phase. The additional term in Eq. (7) facilitates a decrease in the weight of connections between the input and cortical layers. This downscaling occurs in proportion to the firing activity of post-synaptic neurons; as their firing rates increase, their synaptic connection strengths decrease. Conversely, the first term in the equation prevents complete downscaling of synaptic strengths, preserving connections that share pixels with other cortical neurons encoding different images but of the same label.

In Fig. 5B, we illustrate the distribution of connection weights post-sleep for zeros and ones. Despite neurons encoding zeros exhibiting a larger number of nonzero connections, their average weights are lower than those encoding ones. This equilibrium in weights enables us to maintain consistent average cortical activities across varying input intensities, consequently reducing the number of misclassifications.

3.3. Generalizability

The selection of a leaky neuron is motivated by a higher biological plausibility. To assess the generalizability of our model with different spike generation mechanisms in neurons simpler to model, we repeated our simulations using a single Integrate-and-Fire (IF) neuron instead of a Leaky Integrate-and-Fire (LIF) neuron. (Fig. 6).

3.4. Testing on CL scenarios

Fig. 7 top left panel illustrates the results of our model on the Split MNIST. Split MNIST is a CL scenario where, in each experience, the model learns two new classes without forgetting previously learned ones. In the first experience, we train the model on digits zero and one and test on zeros and ones; in the subsequent experiences, we train the network on digits two and three, and so forth. We utilize a batch size of 50 images per label. Each point in the figure represents an average over 50 trials of the test set (comprising 500 randomly chosen images). We use the same parameters as defined in the previous section. Fig. 7 top right panel depicts the results of our model on Rotational MNIST. In this scenario, all labels are available from the first experience, and in successive experiences, digits are rotated progressively from 0° to 90°. We utilize a batch size of 50 images per

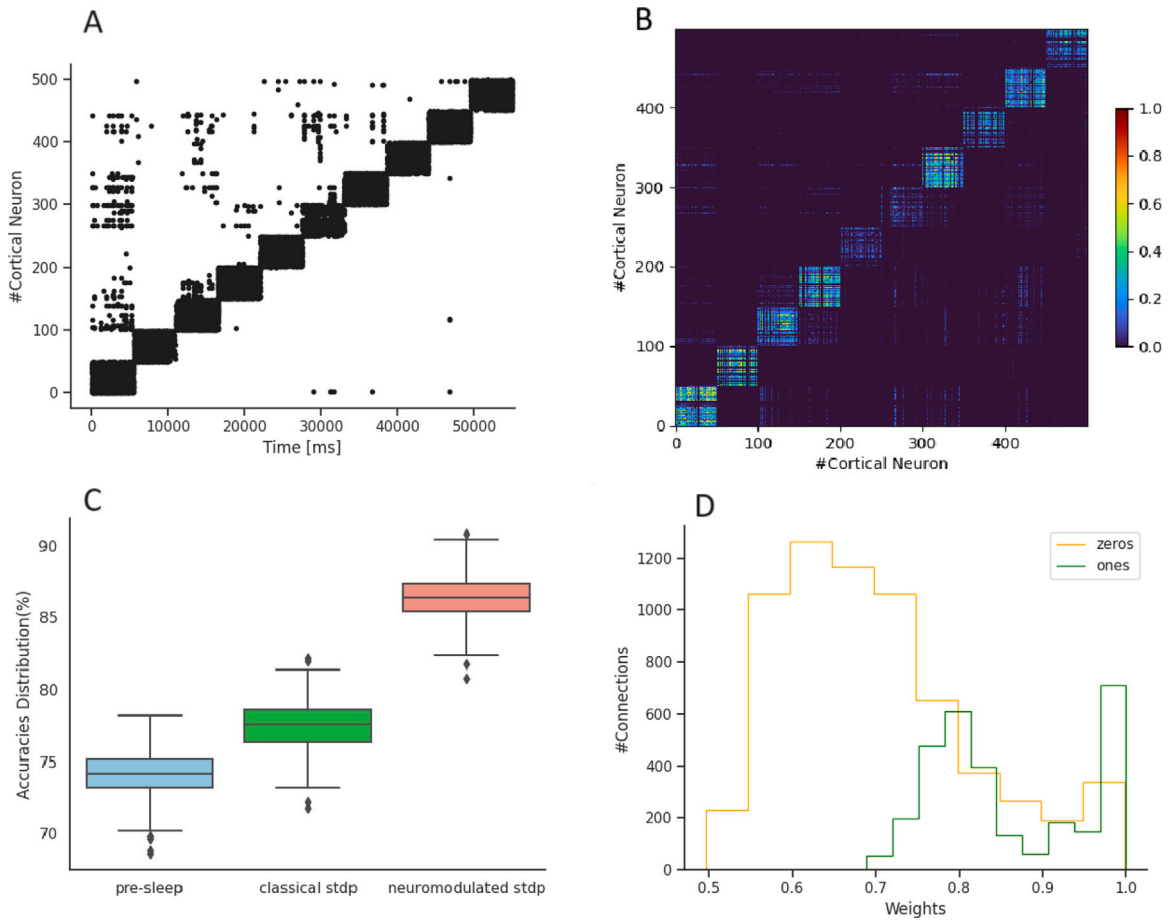

Fig. 5. **A**: Raster plot of neocortical neurons during the sleep phase. For clarity the replay has been ordered. **B**: Connections of neocortical neurons after the sleep phase. **C**: Accuracies distributions comparison between no sleep (blue), classical stdp (green, same rule used in [44]) and neuromodulated (red). Number of test trials:500, randomly taken **D**: Weights distributions between neocortex and input layer after the sleep phase. Each bin has been averaged over three trials.

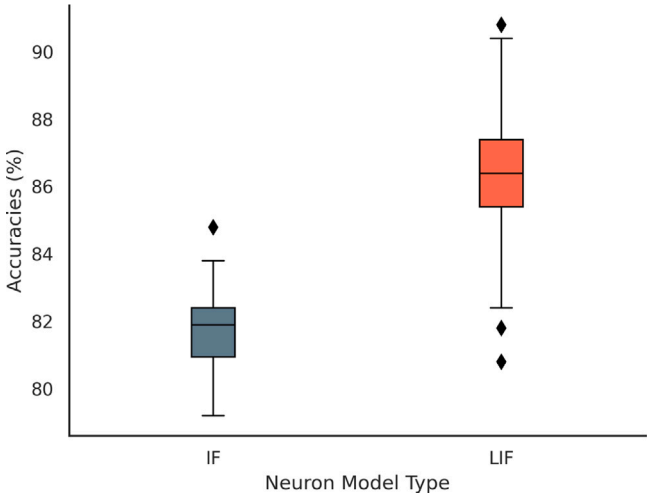

Fig. 6. Accuracies distribution comparison with two different single neuron models. Number of test trials:500, randomly taken.

label. Each point in the figure represents an average over 50 trials of the test set (comprising 500 randomly chosen images). We utilize the same parameters as found in the previous section, except for parameters dependent on the network size, which are properly rescaled. We test the model after each experience on old and current rotations. Our model achieved a 93.9% average accuracy over the experiences on the Split MNIST and a 82.4% on Rotational MNIST to be compared with the 83.2% and 81.8% accuracy achieved by the PNN. We also tested our model on the CIFAR10 and CIFAR100 datasets (Fig. 7, bottom panels). In the first experience, we trained the model using only the first 2 classes for CIFAR10 and the first 20 classes for CIFAR100. In each subsequent experience, we introduced 2 new classes for CIFAR10 and 20 for CIFAR100. During every evaluation phase, both our model and PNN were tested on all previously learned classes as well as the newly introduced ones. Our model achieved average accuracies of 65.3% and 29.4% on CIFAR10 and CIFAR100 to be compared with the 76% and 47.6% average accuracies achieved by PNN.

3.5. Testing on gripper data

To collect sensor signals from various objects, we use a soft pneumatic gripper equipped with four sensors, secured together using stretchable nylon thread as shown in Fig. 8. We employ commercially available flex sensors to measure finger bending, and a force-sensitive resistor (FSR) to quantify the force applied at the fingertip.

The outputs from these flex and force sensors are sent to an Arduino Due board, which is connected to a computer for further processing and analysis. We conduct measurements on 14 different objects: a solid cylinder, hollow cylinder, gluestick, plier, manometer, watch, rectangular block, cube, earpod, mobile phone, earpod case, stapler, bottle, and ball. For each object, we collect 50 data points, considering various orientations. During data collection, the gripper repeatedly holds and releases the object at different positions, with each cycle lasting approximately 39 s. Each data point is represented as a 600-dimensional vector (150 data points times 4 sensors), capturing the

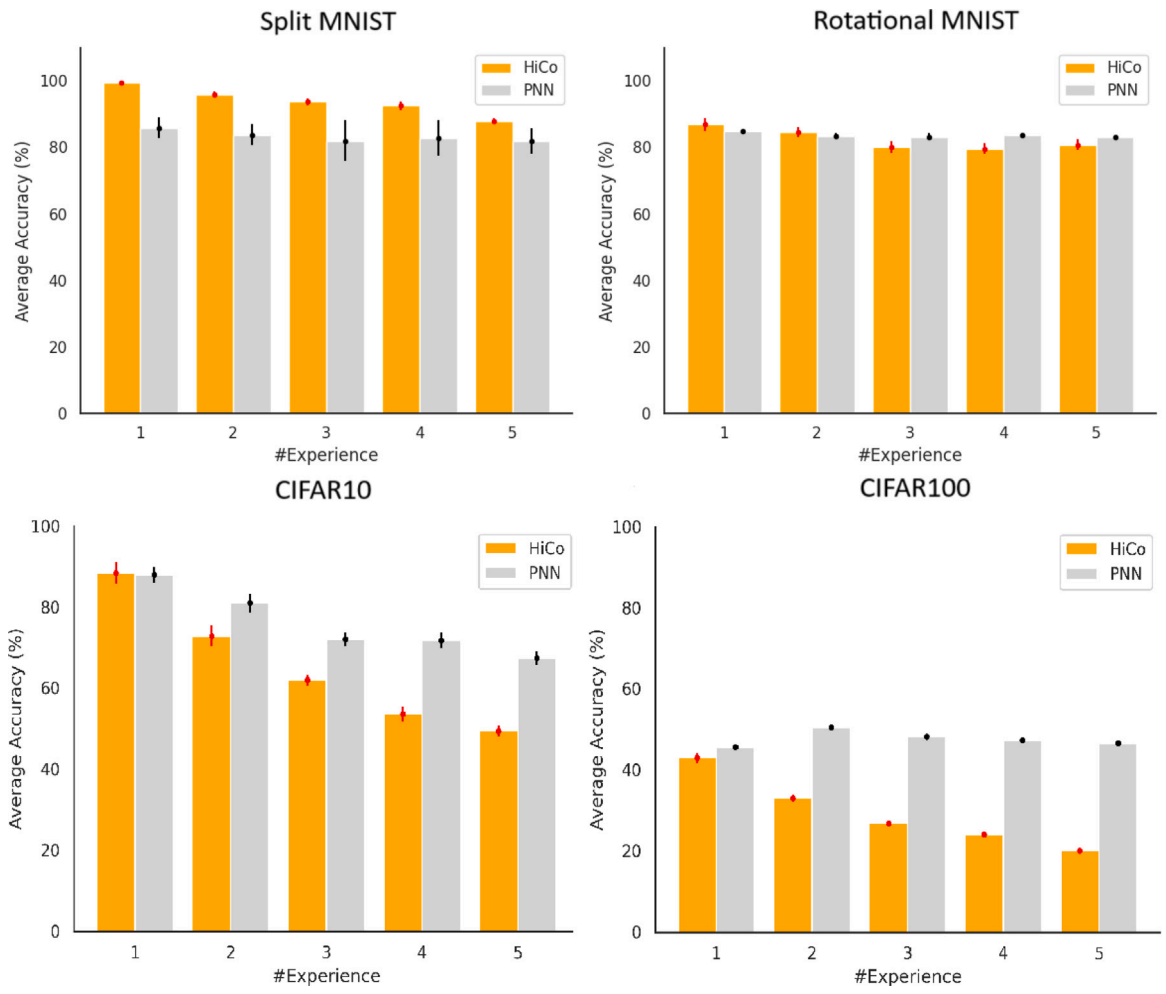

Fig. 7. Evaluation of the proposed model on four different CL scenarios. Each point is averaged over 50 trials of the test set. Rotations were progressive from 0 to 90. During the evaluation phase, never seen data from past and novel experience were used as test set.

Fig. 8. Image of the gripper used and the objects. On the left panel are also visible the four sensor used.

sensor signals recorded during that time interval. Data acquisition for each object takes about 37 min, using a computer equipped with an Intel Core i7 CPU @ 2.80 GHz and GTX 1070 GPU, running Windows 10.

Initially, we attempt to reduce the dataset's dimensionality. For each object class, we calculate the two-point autocorrelation function:

$$f(k) = \frac{1}{(n-k)\sigma^2} \sum_{i=k}^{n} (x_i - \mu)(x_{i-k} - \mu) \tag{11}$$

Here, x represents the sensor readings, k is the delay, μ is the expected value of x, and σ is its variance. The function $f(k)$ indicates the correlation between a point and another point that is k points ahead. We compute the autocorrelation for each class and then average it across all classes. The result is shown in Fig. 9B, where we observe that the autocorrelation function reaches zero at $k \approx 30$, which is around ≈ 8 seconds. Hence, we decide to select one out of every 30 points from each sensor acquisition. Subsequently, we one-hot-encode each value of the remaining 20 points per object into a 10-value vector, resulting in a final input vector of 200 features. Each active feature is then converted into a 500 Hz Poisson spike train, and our data are ready to be input into our spiking neural network.

The data are partitioned into 30 points for the training set, 10 for the validation set, and 10 for the test set. The network is trained on the entire training set, and optimal hyperparameters are identified through

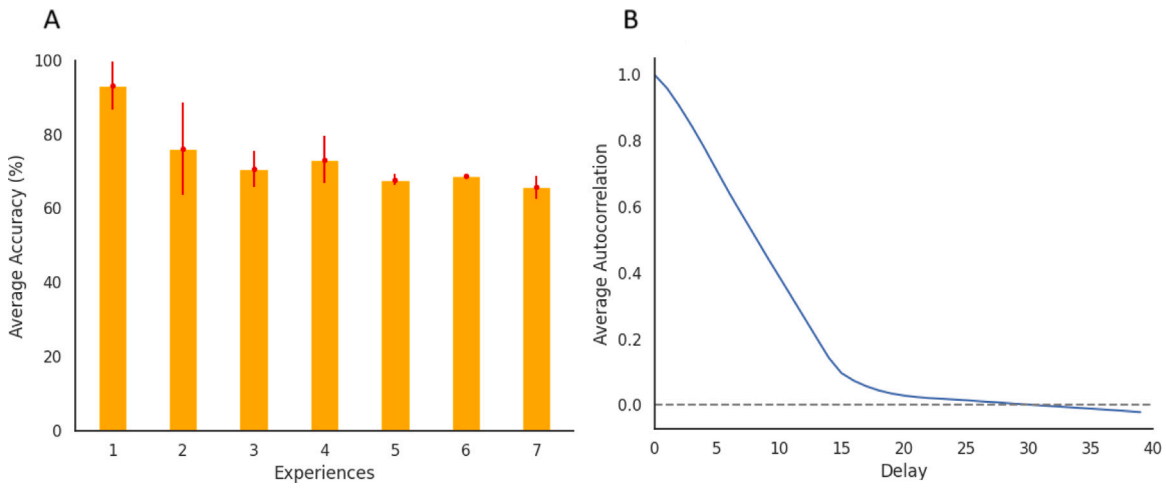

Fig. 9. **A**: Average accuracy for each experience. Each point is averaged over 3 trials, where labels order was randomly shuffled. **B**: Average two-point autocorrelation. The average is over objects and labels. The delay is computed in steps.

testing on the validation set. The search range for the hyperparameters remains consistent with the previous section. A Bayesian search identifies a small parameter set that achieves 70% accuracy on the validation set. The parameter values are $W_{m,sleep} = 0.006$, $g_c = 1.1$ nS, and $tar = 5$.

Subsequently, the network is incrementally trained, introducing two new classes at each experience. In Fig. 9A, we observe the performance of our model evaluated on the test set. Each point represents an average over 3 trials where we randomly shuffle the order of labels at each experience. The average accuracy over all the experiences is 73.6%

4. Conclusion & discussion

It is known that sleep that follows the exposure to experiences progressively transforms them into more abstract, semantic memories [4]. These memory consolidation processes enable us as humans to continually acquire new knowledge and integrate new information. This is also a vital characteristic for a machine that aims to continually learn from a stream of experiences over time. Among the factors contributing to this transformation are the replays in the hippocampus, that triggers the reactivation and redistribution of synaptic connections in the neocortex. This reactivation process allows episodic and specific memories to be integrated and converted into more general and semantic memories. However, the precise mechanism supporting this process and the selection of the memories to be replayed is still under investigation. This modeling work is inspired by the Integrative Theory of consciousness [10], which leverages the apical mechanisms experimentally demonstrated by [11] in wakefulness and discussed for dreaming [12,13] unconscious states and create a coherent systemic view based on the Dendritic Integration Theory [14]. In such a systemic theory an essential ingredient is the interplay between contextual signals projected by other areas strongly modulating the local activity. In this study, we developed a spiking neural network composed of several partitions arranged in a closed-loop. Each partition represents at an extreme level of abstraction the function in action in three different cerebral macro-areas (hippocampus, semantic and perceptual cortical areas). Not withstanding the high level of abstraction, the parameters of the neuronal, synaptic and plasticity dynamics have been set to realistic values. The proposed model involves a two-step learning process. In the first phase, the network encodes unseen instances as episodic memories, facilitated by the presence of the time-dependent contextual signals that modulates cortical neurons activity (see Fig. 2, U_{perc}, U_{cue} and Λ_{sema}) and a global brain-state dependent neuromodulatory signal. During the second phase, hippocampal reactivation is propagated towards the other two areas. Only neocortical neurons that receive the context-specific signal undergo plasticity and support the redistribution of connections with the input layer. We emphasize that we did not aim to construct a detailed model of the interaction between the hippocampus and neocortex, but rather kept the computational complexity to a minimum. This was primarily because we wanted the model to be quick in learning and recognizing a substantial amount of data. For this reason, we chose to modulate through contextual projectors the activity of simple LIF neuron, instead of including a multi-compartment neuron model supporting apical-amplification in its detailed dynamics. This choice reduced the computational cost. We also constructed a highly simplified version of the hippocampus, which lacks the presence of inhibitory neurons and cannot generate any oscillation. Our hippocampus was inspired by the work of [40] and its sole role is to recall episodic memories and their labels. The activation of the input layer during the sleep phase is essential for the semantization process we aimed to explore (see Fig. 3). A more biologically complete framework would require the inclusion of the thalamus, as evidence suggests that the co-activation of the thalamus, hippocampus, and cortex plays a crucial role in nightly memory replay [4]. In a more realistic model, thalamo-cortical connections would enable the thalamus to activate itself via top-down pathways [19]. However, we did not model the thalamus in our study, as doing so would have significantly increased the complexity and computational cost of our simulations. To approximate this mechanism, we introduced a feedback connection between the hippocampus ($CA3_{image}$ population) and the input layer, effectively simulating thalamic activation. This design choice allowed us to maintain the core dynamics of memory consolidation while keeping the model computationally tractable.

We tested our model on CL scenarios such as Split and Rotational MNIST, CIFAR10 and CIFAR100. We compared our model's performance with that of a PNN trained on the same data. As can be noticed in Fig. 7 our model performed comparably or slightly better than PNN on MNIST, but it was outperformed by PNN on the CIFAR datasets. This discrepancy it is due to Task ID parameter (as already mentioned in the Method section) used by PNN. This parameter provides a significant advantage, particularly on CIFAR100, where the model only needs to classify among 20 classes per experience, whereas our model must handle an increasing number of classes over time. We also compared our model's performance with that of the work by [19], although we did not present the results explicitly. Our model's performance is comparable to theirs, with lower variability.

The future directions of this work are twofold. One direction is to expand and enhance the proposed model by including partitions representing thalamic function. In particular, the Thalamic nuclei specific for each sensorial modality still engage with the corresponding cortical areas during deep-sleep, while non specific thalamic nuclei

transport contextual input from other areas during REM sleep and awake day-dreaming. The second direction is to make the model more suitable for a robotic application. SNN are considered to be the third generation of neural network. Even if their performance are still behind deep learning state-of-art there are promising feature that make them appealing. They could result in great energy performance and faster response when implemented on a neuromorphic hardware such as SpiNNaker [47], NeuroGrid [48] etc. The proposed model would excel in a multi-input scenario, thanks to the hippocampus that can link representation in different part of the neocortex (such as visual and motor cortex). Finally, we emphasize that while our model was successfully trained on sensory data from a soft pneumatic gripper, this was only possible due to a post-processing step that transformed the temporal signals into static representations. As a consequence, our current approach is not inherently suited for datasets that require direct event-based processing. We acknowledge the importance of testing on event-based datasets, and future work could explore integrating direct event processing into our framework.

CRediT authorship contribution statement

Federico D'Alba: Writing – original draft, Validation, Software, Methodology, Conceptualization. **Nilay Kushawaha:** Software, Data curation. **Lorenzo Fruzzetti:** Conceptualization. **Pier Stanislao Paolucci:** Writing – review & editing. **Egidio Falotico:** Supervision.

Declaration of Generative AI and AI-assisted technologies in the writing process

During the preparation of this work, the authors used ChatGPT 4.0 in order to improve the readability and language of the manuscript. After using this tool/service, the authors reviewed and edited the content as needed and take full responsibility for the content of the published article.

Declaration of competing interest

The authors declare the following financial interests/personal relationships which may be considered as potential competing interests: Federico D'Alba reports financial support was provided by EBRAINS AISBL. If there are other authors, they declare that they have no known competing financial interests or personal relationships that could have appeared to influence the work reported in this paper.

Acknowledgments

This work was supported by Italian National Recovery and Resilience Plan (NRRP), M4C2, funded by European Union–NextGenerationEU (ProjectIR0000011,"EBRAINS-Italy")underGrantCUPB51E22000150006 (supporting FDA, NK, EF).

This work has been cofunded by the European Next Generation EU through Italian MUR grant CUP I53C22001400006 (FAIR PE0000013 PNRR Project, supporting PSP).

Data availability

Data will be made available on request.

References

[1] L. Squire, N. Cohen, Nadel, The medial temporal region and memory consolidation: a new hypothesis, Mem. Consol.: Psychobiol. Cogn. (1984) 185–210.

[2] L. Nadel, A. Samsonovich, L. Ryan, M. Moscovitch, Multiple trace theory of human memory: computational, neuroimaging, and neuropsychological results, Hippocampus 10 (2000) 352–368, http://dx.doi.org/10.1002/1098-1063(2000)10:4<352::AID-HIPO2>3.0.CO;2-D.

[3] G. Winocur, M. Moscovitch, Multiple trace theory of human memory: computational, neuroimaging, and neuropsychological results, J. Int. Neuropsychol. Soc. 17 (2011) 766–780, http://dx.doi.org/10.1017/S1355617711000683.

[4] J. Klinzing, N. Niethard, J. Born, Mechanisms of systems memory consolidation during sleep, Nature Neurosci. 22 (2019) 1598–1610.

[5] L. Genzel, J. Rossato, J. Jacobse, R. Grieve, P. Spooner, F. Battaglia, G. Fernández, R. Morris, The yin and yang of memory consolidation: Hippocampal and neocortical, Plos Biology (2011) http://dx.doi.org/10.1371/journal.pbio.2000531.

[6] L. Nadel, M. Moscovitch, Memory consolidation, retrograde amnesia and the hippocampal complex, Curr. Opi. Neurobiol. 2 (1997) 217–227, http://dx.doi.org/10.1016/s0959-4388(97)80010-4.

[7] J. McClelland, B. McNaughton, R. O'Reilly, Why there are complementary learning systems in the hippocampus and neocortex: insights from the successes and failures of connectionist models of learning and memory, Phsycol. Rev. 3 (1995) 419–457, http://dx.doi.org/10.1037/0033-295X.102.3.419.

[8] S. Gais, G. Albouy, M. Boly, P. Peigneux, Sleep transforms the cerebral trace of declarative memories, Proc. Natl. Acad. Sci. USA 104 (2007) 18778–18783, http://dx.doi.org/10.1073/pnas.0705454104.

[9] L.R. Squire, L. Genzel, J.T. Wixted, R. G. Morris, Memory consolidation, Cold Spring Harb Perspect Biol. 7 (2015) http://dx.doi.org/10.1101/cshperspect.a021766.

[10] J.F. Storm, P.C. Klink, J. Aru, W. Senn, R. Goebel, A.P.P. Avanzini, W. Vanduffel, P.R. Roelfsema, M. Massimini, M. Larkum, C. Pennartz, An integrative, multiscale view on neural theories of consciousness, Neuron 112 (2024) 1531–1552, http://dx.doi.org/10.1016/j.neuron.2024.02.004.

[11] M. Larkum, A cellular mechanism for cortical associations: an organizing principle for the cerebral cortex, Trends Neurosci. 36 (2012) 141–151, http://dx.doi.org/10.1016/j.tins.2012.11.006.

[12] J. Aru, F. Siclari, W. Phillips, J. Storm, Apical drive-A cellular mechanism of dreaming? Neurosci Biobehav. Rev. 119 (2020) 440–455, http://dx.doi.org/10.1016/j.neubiorev.2020.09.018.

[13] J. Aru, M. Suzuki, M. Larkum, Cellular mechanisms of conscious processing, Trends Cogn. Neurosci. 24 (2020) 814–825, http://dx.doi.org/10.1016/j.tics.2020.07.006.

[14] W.A. Phillips, The Cooperative Neuron: Cellular Foundations of Mental Life, Oxford University Press, ISBN: 9780198876984, 2023, http://dx.doi.org/10.1093/oso/9780198876984.001.0001, URL.

[15] S. Diekelmann, J. Born, The memory function of sleep, Nat. Rev. Neurosci. (2010) 114–126, http://dx.doi.org/10.1038/nrn2762.

[16] A. Takashima, I. C. Nieuwenhuis, O. Jensen, L. Talamini, M. Rijpkema, G. Fernández, Shift from hippocampal to neocortical centered retrieval network with consolidation, J Neurosci. (2009) 12–29, http://dx.doi.org/10.1523/JNEUROSCI.0799-09.2009.

[17] D. Kumaran, D. Hassabis, J. McClelland, What learning systems do intelligent agents need? Complementary learning systems theory updated, Trend Cogn. Sci. (2016) 512–534, http://dx.doi.org/10.1016/j.tics.2016.05.004.

[18] C. Capone, E. Pastorelli, B. Golosio, P.S. Paolucci, Sleep-like slow oscillations improve visual classification through synaptic homeostasis and memory association in a thalamo-cortical model, Sci. Rep. 9 (2019) http://dx.doi.org/10.1038/s41598-019-45525-0.

[19] B. Golosio, C. De Luca, C. Capone, E. Pastorelli, G. Stegel, G. Tiddia, G. De Bonis, P.S. Paolucci, Thalamo-cortical spiking model of incremental learning combining perception, context and NREM-sleep, PLoS Comput. Biol. (2021) http://dx.doi.org/10.1371/journal.pcbi.1009045.

[20] G. Tononi, C. Cirelli, Sleep and the price of plasticity: From synaptic and cellular homeostasis to memory consolidation and integration, Neuron (2015) http://dx.doi.org/10.1016/j.neuron.2013.12.025.

[21] C. Puentes Mestril, S. Aton, Linking network activity to synaptic plasticity during sleep: Hypotheses and recent data, Front. Neural Circuits (2017) http://dx.doi.org/10.3389/fncir.2017.00061.

[22] W. Gerstner, W. Kistler, R. Naud, L. Paninski, Neuronal Dynamics: From Single Neurons to Networks and Models of Cognition, Cambridge University Press, 2014.

[23] G. Carpenter, S. Grossberg, The ART of adaptive pattern recognition by a self-organizing neural network, IEEE (1988) http://dx.doi.org/10.1109/2.33.

[24] N. Frémaux, W. Gerstner, Neuromodulated spike-timing-dependent plasticity, and theory of three-factor learning rules, Front. Neural Circuits 2 (2016) http://dx.doi.org/10.3389/fncir.2015.00085.

[25] C. Ranganath, G. Rainer, Neural mechanisms for detecting and remembering novel events, Nat Rev Neurosci. (2003) http://dx.doi.org/10.1038/nrn1052.

[26] L.A. Atherton, D. Dupret, J.R. Mellor, Memory trace replay: the shaping of memory consolidation by neuromodulation, Trends Neurosci. 38 (2015) 560–570, http://dx.doi.org/10.1016/j.tins.2015.07.004.
[27] J.E. Lisman, A.A. Grace, The hippocampal-VTA loop: controlling the entry of information into long-term memory, Neuron 46 (2005) 703–713, http://dx.doi.org/10.1016/j.neuron.2005.05.002.
[28] T. Lesort, V. Lomonaco, A. Stoian, D. Maltoni, D. Filliat, N. Rodríguez, Continual learning for robotics: Definition, framework, learning strategies, opportunities and challenges, 2019, http://dx.doi.org/10.48550/arXiv.1907.00182, arXiv.
[29] N. Kushawaha, L. Fruzzetti, E. Donato, E. Falotico, SynapNet: A complementary learning system inspired algorithm with real-time application in multimodal perception, IEEE Trans. Neural Networks Learn. Syst. (2024) 1–15, http://dx.doi.org/10.1109/TNNLS.2024.3446171.
[30] D. Singh, K.A. Norman, A.C. Schapiro, A model of autonomous interactions between hippocampus and neocortex driving sleep-dependent memory consolidation, PNAS 119 (2022) http://dx.doi.org/10.1073/pnas.2123432119.
[31] M.W. Remme, U. Bergmann, D. Alevi, S. Schreiber, H. Sprekeler, R. Kempter, Hebbian plasticity in parallel synaptic pathways: A circuit mechanism for systems memory consolidation, PLoS Comput. Biol. (2021) http://dx.doi.org/10.1371/journal.pcbi.1009681.
[32] A.B. Lehr, J. Luboeinski, C. Tetzlaff, Neuromodulator-dependent synaptic tagging and capture retroactively controls neural coding in spiking neural networks, Nature (2022).
[33] N. Chrysanthidis, F. Fiebig, A. Lansner, P. Herman, Traces of semantization, from episodic to semantic memory in a spiking cortical network model, ENeuro 9 (2022) http://dx.doi.org/10.1523/ENEURO.0062-22.2022.
[34] E. Spens, N. Burgess, A generative model of memory construction and consolidation, Nat. Hum. Behav. 9 (2024).
[35] Y. Kobayashi, K. Murakoshi, A generative model of memory construction and consolidation, Wiley Online Libr. (2007) http://dx.doi.org/10.1002/ecjb.20332.
[36] M.D. Howard, S.W. Skorheim, P.K. Pilly, A model of bi-directional interactions between complementary learning systems for memory consolidation of sequential experiences, Front. Syst. Neurosci. 16 (2022) http://dx.doi.org/10.3389/fnsys.2022.972235.
[37] Y.N. Kenett, M. Faust, A semantic network cartography of the creative mind, Trends Cogn. Sci. 23 (4) (2019) 271–274.
[38] M. Stimberg, R. Brette, D. Goodman, Brian 2, an intuitive and efficient neural simulator, ELife (2019) http://dx.doi.org/10.7554/eLife.47314.
[39] F. Nogueira, Bayesian Optimization: Open source constrained global optimization tool for Python, 2014, URL https://github.com/bayesian-optimization/BayesianOptimization.
[40] D. Casanueva Morato, A. Ayuso Martinez, J. Dominguez Morales, A. Jimenez Fernandez, G. Jimenez Moreno, Bio-Inspired Implementation of a Sparse-Learning Spike-Based Hippocampus Memory Model, IEEE, 2023, http://dx.doi.org/10.1109/ISCAS46773.2023.10181583.
[41] M. Westerlund, L. Pylkkanen, The role of the left anterior temporal lobe in semantic composition vs. semantic memory, Neuropsychologia 57 (2013) 59–70.
[42] C. Capone, C. Lupo, P. Muratore, P.S. Paolucci, Beyond spiking networks: The computational advantages of dendritic amplification and input segregation, Proc. Natl. Acad. Sci. 120 (2023) http://dx.doi.org/10.1073/pnas.222074312.
[43] E. Pastorelli, A. Yegenoglu, N. Kolodziej, W. Wybo, F. Simula, S. Diaz, J.F. Storm, P.S. Paolucci, Two-compartment neuronal spiking model expressing brain-state specific apical-amplification, -isolation and -drive regimes, 2023, arXiv:2311.06074.
[44] P.U. Diehl, M. Cook, Unsupervised learning of digit recognition using spike-timing-dependent plasticity, Front. Comput. Neurosci. (2015) http://dx.doi.org/10.3389/fncom.2015.00099.
[45] A.A. Rusu, N.C. Rabinowitz, G. Desjardins, H. Soyer, J. Kirkpatrick, K. Kavukcuoglu, R. Pascanu, R. Hadsell, Progressive neural networks, 2016, http://dx.doi.org/10.48550/arXiv.1606.04671, arXiv.
[46] K. Simonyan, A. Zisserman, Very deep convolutional networks for large-scale image recognition, 2015, http://dx.doi.org/10.48550/arXiv.1409.1556, arXiv.
[47] S. Furber, F.T. Galluppi, L. Plana, The SpiNNaker Project, vol. 102, 2014, pp. 652–664.
[48] B. Varkey Benjamin, et al., Neurogrid: A mixed-analog-digital multichip system for large-scale neural simulations, IEEE (2014) http://dx.doi.org/10.1109/JPROC.2014.2313565.

Federico D'Alba received his Bachelor's and Master's degrees in Physics from the University of Pisa. He is currently a Ph.D. student at the BioRobotics Institute of Scuola Superiore Sant'Anna in Pisa. His research focuses on the development of spiking neural network models inspired by or functionally resembling specific brain areas, with applications in continual learning. His main areas of interest include spiking neural networks, computational neuroscience, and machine learning.

Nilay Kushawaha received the bachelor's degree in physics from the University of Delhi, Delhi, India, in 2020, and the master's degree in physics from Indian Institute of Technology Indore, Indore, India, in 2022. He is currently pursuing the Ph.D. degree in biorobotics and AI with The Biorobotics Institute, Scuola Superiore Sant'Anna, Pisa, Italy. His current research interests include continual learning, brain-inspired algorithms, reinforcement learning, and control theory.

Lorenzo Fruzzetti received the bachelor's degree in biological science and the master's degree in neuroscience from the University of Pisa, Pisa, Italy, in 2016 and 2019, respectively. He is currently pursuing a postdoc at Consiglio Nazionale delle Ricerche (CNR), Pisa. His current research interests include reinforce ment learning, continual learning, spiking neural networks, brain-inspired algorithms, and data analysis.

Pier Stanislao Paolucci currently coordinates INFN research activities in the bio-inspired Future Artificial Intelligence Research (FAIR) and EBRAINS-Italy projects funded by the Next Generation EU program. Previously, he served as technological research leader of the "Networks underlying cognition and consciousness" activities in the Human Brain Project. He served as CTO of the Diopsis multi-processor Systems-on-Chip design center of a major semiconductor manufacturer. He authored several international patents and invented widely used numerical algorithms for parallel/distributed computing platforms.

Egidio Falotico received the M.S. degree in computer science from the University of Pisa, Pisa, Italy, in 2008, the Ph.D. degree in biorobotics from Scuola Superiore Sant'Anna (SSSA), Pisa, in 2013, and the Ph.D. degree in cognitive science from University Pierre et Marie Curie, Paris, France, in March 2013. He is currently an Assistant Professor with SSSA, The BioRobotics Institute. He is currently the Deputy Leader and the Publications Manager in the Sub-Project 10 of the Human Brain Project. He is the author or co-author of more than 40 international peer-reviewed papers. He regularly serves as a reviewer for more than ten international ISI journals. He has been involved in some EU-funded projects (I-SUPPORT, SWARMs, SMARTE, RoboSoM, and RobotCub), focusing on the development of brain-inspired algorithms for robot control. His research interests focus on neurorobotics, i.e., the implementation of brain models from neuroscience in robots.